



HAL
open science

Trends in mechanical and electrical properties for hard-soft nano-phased metallic alloys

Solène Iruela, Fabien Volpi, Annie Antoni-Zdziobek, Vincent Jarry, Yannick
Champion

► **To cite this version:**

Solène Iruela, Fabien Volpi, Annie Antoni-Zdziobek, Vincent Jarry, Yannick Champion. Trends in mechanical and electrical properties for hard-soft nano-phased metallic alloys. *Materials Today Communications*, 2023, 35, 10.1016/j.mtcomm.2023.106292 . hal-04210923

HAL Id: hal-04210923

<https://cnrs.hal.science/hal-04210923>

Submitted on 19 Sep 2023

HAL is a multi-disciplinary open access archive for the deposit and dissemination of scientific research documents, whether they are published or not. The documents may come from teaching and research institutions in France or abroad, or from public or private research centers.

L'archive ouverte pluridisciplinaire **HAL**, est destinée au dépôt et à la diffusion de documents scientifiques de niveau recherche, publiés ou non, émanant des établissements d'enseignement et de recherche français ou étrangers, des laboratoires publics ou privés.

Trends in mechanical and electrical properties for hard-soft nano-phased metallic alloys.

Solène Iruela ^{1,2}, Fabien Volpi ¹, Annie Antoni-Zdziobek ¹, Vincent Jarry ² and Yannick Champion ¹

1. Univ. Grenoble Alpes, Grenoble INP, CNRS, SIMaP, 38000 Grenoble, France.

2. METALOR, rue des Aquées, 28190 Courville-sur-Eure, France

Corresponding author: yannick.champion@simap.grenoble-inp.fr

Abstract

Separate modeling of the mechanical and electrical behaviors is proposed with dependence on the microstructure, volume fraction and the nature of phases in the AgCuPd ternary system. The objective is to assess trends in terms of performances for applications where combination of the mechanical strength and electrical conductivity is to be optimized. The two models are linked and compared to experimental measurements, to evaluate the mechanical-electrical couple on the performances and the limits. The analysis brings insight of the physical and microstructural parameters governing properties for a better understanding of the behavior.

Keywords

Mechanical strength, electrical conductivity, hard soft phases, AgCuPd, nanophase,

Introduction

Improving both high strength and high electrical conductivity of metallic alloys is one of the key challenges to gain in integrity of electric and electronic devices such as connectors, switches, lead frames, wires, and so on, used in transportation and aerospace, housing, communication, ... Gliding contact for example must show good wear and plastic deformation resistance as well as good electrical conductivity for decreasing the working current density. However, evolution of these two properties is antagonist whatever most of the materials strategy adopted. Improving strength needs adding defects to the metal which limits dislocation displacements but produces also electron scattering then decreasing electrical conductivity (and vice versa). The two main strategies for strengthening consist in solid solution and precipitation hardening. The first one leads to a hyperbolic dependence of strength as a function of the electrical conductivity (corresponding to an initial low strengthening for a large degradation of conductivity) and the trend for the second strategy is a linear (negative) dependence [1, 2]. In some cases, as for wires processed by drawing, fine-grained microstructure is formed. Additional Hall-Petch effect has to be considered and it has been observed a linear dependence similar to precipitation hardening for grain refinement [3], except for large fractions of nano-twin boundaries which

produce combined high strength and electrical conductivity [4]. Singularly, relevant combination in copper of fine grains and low volume fraction of Cr hard nano-precipitates is able to produce both desirable trends [5]. Over the domain of the alloy composition, two types of strategy are identified corresponding to two communities of users. A first one is concerning those who need predominantly high conductivity obtained with low alloyed metals and will attempt to strengthen them. Examples are the solid solution and the precipitation hardening (for example Cu 0.15 wt%Sc or Cu 0.15wt%Zr with 300 MPa and 90% IACS)[6, 7]. The second is concerning those who need predominantly high mechanical strength obtained with concentrated alloys and will attempt to increase their electrical conductivity. An emblematic example is Cu 2 wt%Be (9 volume % of Be) which exhibits 1200 MPa and 25% IACS [8, 9]. It is emphasizing here that the two communities are dealing with different objectives and then material design orientations.

The work presented in this article concerns highly concentrated alloy composites formed by phase separation in the AgCuPd ternary system, leading to mixing of mechanically soft Ag-rich phase and hard CuPd-phase. In such a mixture plasticity occurs in the soft phase. For fine hard phase dispersion with a low volume fraction, the hard phase has the role of blocking the dislocations. Hardening then results from the bending of dislocations and ultimately a bypass of the precipitate (Orowan mechanism). In the case of mixing phases with comparable volume fraction and size, the mechanism is different. The plastic strain in the soft phase at a rigid front of a hard phase generates a strain gradient to which a back stress is associated, opposite to the direction of the applied stress. This effect has been analyzed by Ashby [10] and used to explain many cases of soft-hard phase effects (indentation, deformation of small objects ...). For instance, strain gradient allowed to analytically model the deformation in an aluminum - zirconium based metallic glass composites with micrometric microstructure sizes and to explain the variations in mechanical resistance with the volume fraction of phases [11]. As the AgCuPd alloy studied is processed by wire drawing, the Ag(Pd) and CuPd phases are nanometric. It was verified that the law derived by Perrière et al [11] does not satisfy the variations of experimental stresses measured with the volume fractions of nanometric phases. To explain these variations, an Hall-Petch type effect has been added. It is recalled that the Hall-Petch effect persists in metals up to largely submicron grain sizes (25 nm for Cu, 10 nm for Ni). A model for the electrical property is also proposed to evaluate trends in the combination of mechanical strength and electrical conductivity.

Processing, microstructure and measurements

Specimens were prepared and processed into wire form to produce the microstructure and the phases as close as possible to those of the materials used in applications. High purity Ag, Cu, Pd were melted by radio frequency induction in an alumina crucible, under He atmosphere. The liquid alloys were

maintained at 1570°C during 15 minutes to insure a good mixing achieved by electromagnetic stirring. As prepared alloys were then laminated to produce bars, with size in the range of few centimeters and finally drawn to form wires with diameter in the range of 60 μm. Drawing is a repeated plastic deformation process and fine grain microstructure (at the submicrometer-scale) as well as high distortion levels (extreme strain hardening) are expected. AgCuPd ternary alloy is characterized by a complex phase diagram.

Three phases with compositional fluctuation can be formed depending on thermal treatment: the Ag(Pd) solid solution, the Cu-Pd intermetallics disordered A1 (face centered cubic) and ordered B2 (simple cubic).

The formation of the CuPd-B2 phase is desired for its far better electrical properties compared to CuPd-A1 phase, which would improve the overall wire conductivity [12]. However, it is well known that the A1 – B2 transformation is very slow and need long-lasting high temperature annealing [13]. Best compromise in term of annealing is rather tedious to define as such a process would reduce lattice distortion to improve ductility, keep small grain size for high strength and form the largest fraction of B2 phase to improve electrical conductivity. The objective of this work is to analyze the combined effects of the microstructure and the phases on the mechanical and electrical properties and shed light on possible optimization or reasonably accessible conditions. For the A1 – B2 transformation study, the alloys were annealed under inert atmosphere at respectively 550°C during 3 months and 725°C during one month. For the analysis presented here, various thermal treatments on the wires, reported in the table 1, were applied to form the relevant microstructure and phases. Three alloys were prepared with composition (table 1) producing various fraction of Ag(Pd), CuPd A1 and B2 phases.

Table 1 : alloys elemental composition, drawing and thermal treatment.

Alloy (at %)	Ag	Cu	Pd	Strain hardening (rate %)	Annealing Temperature (°C)	Time (mins)
1	37.5 ± 2.5	37.5 ± 2.5	27.5 ± 2.5	88	550	2
2	45.5 ± 0.5	29.5 ± 0.5	24.5 ± 0.5	99.5	430	30
3	59.5 ± 0.5	23.5 ± 0.5	16.5 ± 0.5	99.9	400	30

Figure 1 illustrates the microstructural characteristics of the three AgPdCu alloys, showing the presence of Ag(Pd) (initially Ag₈₀Pd₂₀) solid solution, and CuPd in the A1 and B2 forms. The average volume fraction are estimated, for alloy 1 (a) 53% Ag(Pd), 42% CuPd A1 and 5% CuPd B2. For alloy 2 (b) 70% Ag(Pd), 23 % CuPd A1 and 7% CuPd B2. For alloy 3 (c) 83% Ag(Pd), 17% CuPd A1 and CuPd B2 is not detected. Due to foils thickness and surface observations, larger fractions are overestimated and must be corrected using the Schwartz-Saltykov estimate in the range of 10% with additional 10% error [14].

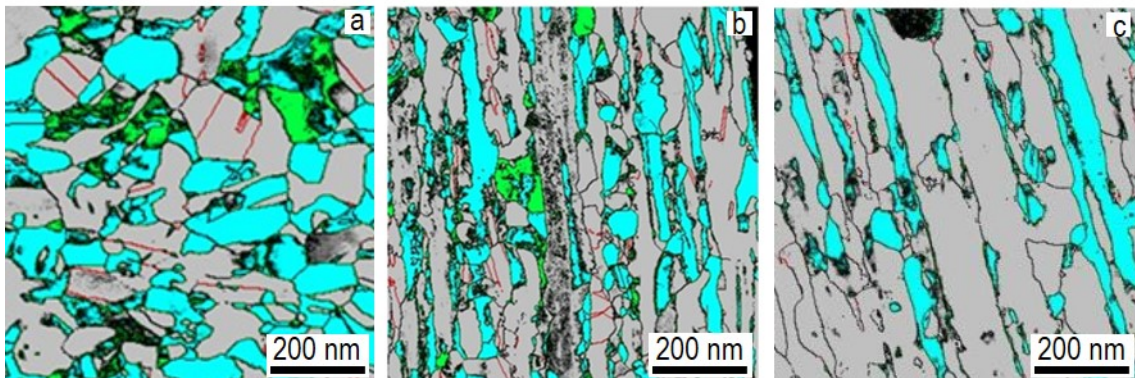


Figure 1. TEM-ACOM imaging of the three alloys reported in the table 1 (respectively a for 1, b for 2 and c for 3), with respectively grey for Ag(Pd) solid solution, blue for CuPd A1 phase and green for CuPd B2 phase. The red lines are twin boundaries, about 5% of the grain boundaries.

Mechanical strength of wires was evaluated by tensile test machine (INSTRON) with specific jaws for wires. Local hardness and elastic modulus of the various phases were obtained using nano-indentation (InForce 50 actuator from Nanomechanics-KLA). Electrical resistivity was measured by the 4-points method on the wires using a home-made test bench. X-ray diffraction (X'Pert Pro Multi purpose Diffractometer PaNalytical) was performed to identify phases and to evaluate grain size from Williamson-Hall and Halder-Wagner line broadening analyses. The microstructure and the phase distribution were imaged using transmission electron microscopy (MET FEG JEOL 2100F) and automated crystal orientation mapping (ACOM) procedure. Modelling of the mechanical strength and electrical conductivity are based on the knowledge of the phases, their distribution and sizes.

In the following, one denotes the soft phase Ag(Pd) solid solution with the subscript s and the hard phase CuPd with the subscript h . For the sake of simplicity, one keeps this notation for the electrical modeling. A linear combination weighted by the fraction of A1 and B2 is used for calculation of properties of the CuPd "hard" phase.

Models

Mechanical strength

The strength at the elasto-plastic transition is modelled as a function of the soft and hard phase fraction and the grain size. The mixing law gives the elastic shear deformation $\gamma = \chi_s \gamma_s + \chi_h \gamma_h$ with respectively the volume fractions and deformations of the soft χ_s, γ_s and hard χ_h, γ_h phases. At the maximum of elastic deformation, elastic relaxation leading to macroscopic plasticity occurs nearly only in the soft phase and thus: $\gamma \approx \chi_s \gamma_s$. In the elastic domain and until the onset of macroscopic plastic deformation, micro-plasticity occurs in soft phase grains which leads to dislocation pile-up at the grain boundaries, at the basis of the Hall-Petch effect model (size effect on yield strength) [15]. Still relying on the Hall-Petch effect, the model predicts that the stress transmitted by the pile-up in an adjacent grain (activating a dislocation source giving rise to macro plasticity) is an amplification of the applied stress τ , by the number of dislocations in the pile-up, i.e. $n\tau$ (figure 2).

At the elasto-plastic transition, the total elastic deformation in a grain has been relaxed with formation of n dislocations, which writes: $\gamma_s D = nb$, where D is the grain size and b is the dislocation Burgers vector. Using the Hook law with G the elastic modulus of the soft phase, the number of dislocations in a pile-up is given by $n = \tau D / \chi_s G b$ and therefore the stress transmitted in the adjacent grain is:

$$n\tau = \frac{\tau^2 D}{\chi_s G b} \quad (1)$$

At the rigid interface between soft and hard phases, the dislocation pile-up in the soft phase is unable to produce relaxation by dislocations emission in the adjacent hard phase and a back stress τ_b is generated, opposing the overall stress built in the soft phase. The back stress is given by the relation derived from the strain gradient model of Ashby [10]:

$$\left(\frac{\tau_b}{\tau_0}\right)^2 = \frac{l_0 \gamma_s}{D} \quad (2)$$

where respectively τ_0 and l_0 are a stress and a length scale characteristics of the soft phase and $\frac{\gamma_m}{D}$ is the strain gradient.

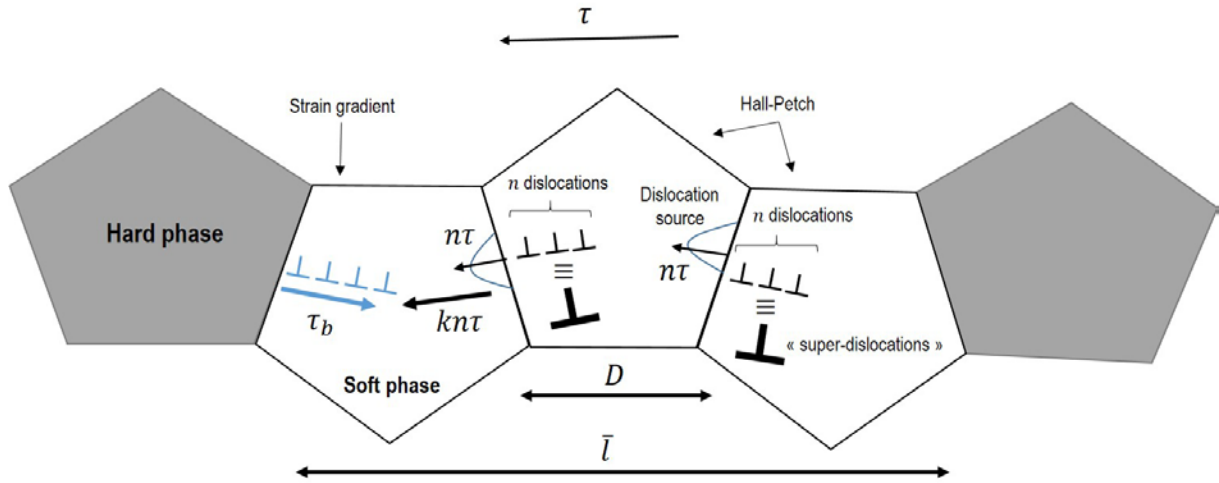


Figure 2: Schematic representation of a microstructural model explaining the mechanical resistance of hard and soft nanophases mixture.

Perrière and Champion showed that equating this back stress with relation (1) gives a good evaluation of the strength variation with the phase volume fraction of the mixing of soft (aluminum) and hard (Zr based metallic glass) with micrometer grain size [11]. However, a large discrepancy is observed when applying this relation to AgCuPd alloys, naturally ascribed to the nanoscale grain size. To take that into account, coupling between soft grains localized in-between successive hard phase grains has been considered. It is assumed that a pile-up of n dislocations in a grain is described by a "super-dislocation" and whose stacking again generates an amplification effect producing at the head a resulting stress $kn\tau$. k is the number of "super-dislocations" in such a secondary pile-up, which is also the number of soft phase grains between two consecutive hard grains. With \bar{l} the average distance between two hard phase grains, $k = \bar{l}/D$. The average distance between two phase grains in a random distribution was calculated by Perrière [11] :

$$\bar{l} = \frac{D_d}{2} \left[\left(8 + \frac{1}{\chi_h} \right)^{1/3} - 2 \right].$$

One thus obtains, assuming the hard and soft phase sizes of the same order of magnitude:

$$kn\tau = \frac{\tau^2 D \left[\left(8 + \frac{1}{\chi_h} \right)^{1/3} - 2 \right]}{2\chi_s Gb} \quad (3)$$

At the elastoplastic transition, the stress defined by the relation (2) is balanced with the back stress at the hard-soft phases interface: $kn\tau = \tau_b$ and then, combining with (1) and (2) the mechanical strength of the phase mixture is obtained:

$$\tau = (\tau_0^2 l_0 G b^2)^{1/3} \times \frac{(4\chi_s)^{1/3}}{\left[\left(8 + \frac{1}{1-\chi_s}\right)^{1/3} - 2\right]^{2/3}} \times \frac{1}{D} \quad (4)$$

To this relation must be added a hypothetical threshold stress, τ_s which would correspond to the extrapolation of the stress for $\chi_s \rightarrow 1$.

$$\tau_e = \tau + \tau_s \quad (5)$$

Electrical conductivity

Many approaches have already been developed to predict the effective conductivity of multi-phased systems: boundary-based approaches (such as the well-known "best-bounds approach" proposed by Hashin & Shtrikman [16]), self-consistent approximation methods, or more empirical approaches that take into account the geometric specificities of the systems under study (percolation, anisotropy, scattering at interfaces,...) [17-20]. Most of these linear approaches combine the individual properties of the constituent phases with their volume fractions. However, none of them are universal as they all rely on strong assumptions related to the geometry of the considered system. Accordingly, the present study proposes to model the AgCuPd system as a 3-dimensional checkerboard structure (3D extension of the 2D-checkerboard approach [21], figure 3a) with a percolated phase (the most conductive one), while scattering at grain boundaries is neglected. An elementary component, reproducing the overall alloy structure by translation, is shown in projection in figure 3b. For the alloy composition considered, the Ag(Pd) (grey) phase is always more than 50% in volume fraction and therefore always percolated. To follow the notation used in the mechanical model, Ag(Pd) is denoted s and the CuPd h .

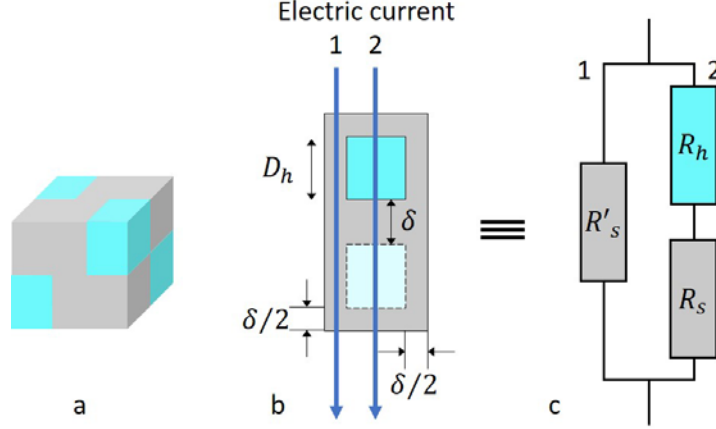


Figure 3: Electric model of the two-phase mixture (more conductive in grey). (a) 3D checkerboard structure with percolation of the most conductive phase. (b) Projection view of the structure with the structural parameters of the modeling. (c) Equivalent electrical circuit.

The average conductivity σ depends only on the resistivity ρ_h, ρ_s , and the volume fractions of the phases. The model in figure 3b is described by an equivalent electric circuit depicted in the figure 3c from which the average conductivity is easily calculated. The characteristic dimensions of each component necessary for calculating the resistance of the circuit in figure 3c are shown in figure 3b (the size of the phase CuPd, D_h and of the spacing between phases CuPd, δ). The average resistivity of the circuit is obtained dividing the resistance by the section of the elementary domain (figure 3b). The calculation is of no particular difficulty. The fraction of one of the phases (arbitrarily CuPd) is introduced in the relation, noting that: $\sqrt[3]{2\chi_h} = 1/(\delta/D_h + 1)$.

The resistivity and therefore the conductivity is given by:

$$\sigma = \frac{1}{\rho} = A \left[\frac{1-(2\chi_h)^{2/3}}{\rho_s} + \frac{2(2\chi_h)^{1/3}}{\rho_h + \rho_s \left(\frac{2}{(2\chi_h)^{1/3}} - 1 \right)} \right] \quad (6)$$

This agrees with $\rho \rightarrow \rho_s$ for $\chi_h \rightarrow 0$. A is a geometric constant, added to account for the difference between the ideal structure in Figure 3a and the actual structure, with a random distribution of phases, their shape and size distribution as observed in Figure 1.

In such mean field geometric model, resistivity of an interface or grain boundaries is easily integrated by adding the corresponding resistances to the two relevant branches in the circuit. However, these contributions were not taken into account, noting that the mean free paths of electrons in the different

phases are smaller than the phase and grain sizes. It is roughly evaluated that the mean free path is of the order of 20 nm for CuPd (B2), 10 nm for Ag(Pd) and below 5 nm for CuPd(A1) [22]. The electrical conductivities vary according to the annealing conditions and the phase formation. The conductivity of the Ag phase will vary depending on its Pd content, and the CuPd phase will vary depending on the rate of B2 formation. Nevertheless, the model considers weak fluctuation in composition and therefore on electrical conductivity.

Experimental comparisons

Mechanical strength

Three alloys were prepared; the volume fraction of Ag(Pd) soft phase and the grain sizes are reported in table 2.

Table 2 : volume fractions are corrected by the TEM foil thickness effect according to [14].

Alloy	σ_e (GPa)	χ_s (%) Ag(Pd)	D_s (nm) Ag(Pd)	D_h (nm) CuPd
1	1.30	48 ± 5	80 ± 9	32 ± 8
2	1.45	63 ± 6	43 ± 6	21 ± 2
3	1.35	75 ± 7	47 ± 4	38 ± 3

According to the Von Mises criterion, the experimental strength is related to the shear strength following, $\sigma_e = \sqrt{3}\tau_e$. The values are plotted as a function of a reduced stress, $\tau_r = \tau/(\tau_0^2 l_0 G b^2)^{1/3}$ in figure 4 and a linear fitting expected according to relation 5 gives : $\sigma_e = 3.94\tau_r + 1.08$.

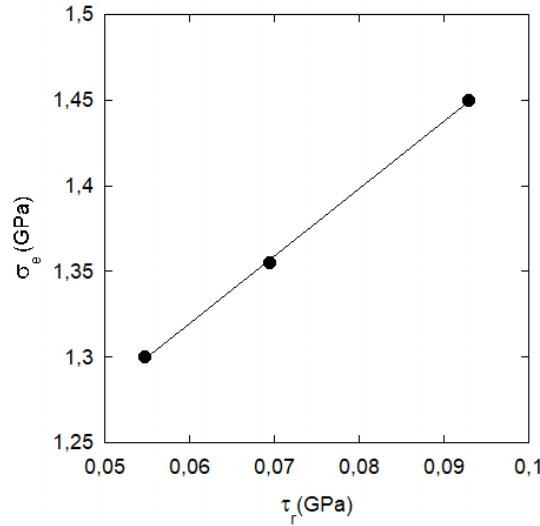


Figure 4: Experimental mechanical strength as a function of the modeled reduced shear strength.

Value of the threshold stress of the order of $\sigma_e \approx 1 \text{ GPa}$, is an extrapolation with no meaning, since it would be that of an hypothetical mixture formed of 100% of nanocrystalline Ag. Obviously the modelling is no longer relevant and diverges smoothly whilst the microstructure changes from soft-hard phases mixture to a dispersion of low fraction of hard particles (Orowan mechanism) and then reaches pure nanocrystalline Ag. Besides, a tensile yield strength for pure nanocrystalline Ag with an average grain size of 13.5 nm was measured of 265 MPa and the ultimate tensile strength is just below 400 MPa [23]. According to equation (4), the fitted slope of 3.94 equals $\sqrt{3}(\tau_0^2 l_0 G b^2)^{1/3}$ which brings some insight on a length scale characterizing the strengthening mechanism. For the soft phase Ag(Pd), the Burgers vector is given by measuring the lattice parameter, of the order of $b = 0.285 \text{ nm}$ ($b = 1/2 \langle 110 \rangle$). The shear modulus is estimated as $G \approx 35 \text{ GPa}$ from nano-indentation measurements. The parameter τ_0 can naturally be associated with a quantity characteristic of the soft phase where the strain gradient is formed. Assuming τ_0 of the order of the resistance of the soft phase confined between hard grains, the value is evaluated by the hardness measured using nano-indentation of the order of 2 GPa . With Tabor's law $H = 3\sigma$, it comes $\tau_0 = H/3\sqrt{3} \approx 0.57 \text{ GPa}$, which gives the length scale of the gradient of the order of $l_0 \approx 13 \text{ nm}$. The physical meaning of this internal length scale is not fully understood. Nevertheless, it is interesting to note that the value evaluated here is close to that measured in other cases where l_0 could be associated with the thickness of the zone where microplasticity occurs in the deformation gradient phenomenon [24]. In this work the values of l_0 for the different alloys studied range from 5.2 to 8.7 nm, which is in reasonable agreement with our finding.

Electrical conductivity

Relation (4) shows that the mechanical properties depend on the volume fraction of soft and hard phases and on the grain size. In contrast, the electrical properties are independent of the grain size, since the mean free path of electrons is lower. They depend on the phase fraction and on the phase composition which determines the electrical conductivity modulated by annealing. After drawing, the alloys are formed of a solid solution of Ag(Pd) with an electrical resistivity of Ag(Pd) ($\text{Ag}_{80}\text{Pd}_{20}$), $\rho_s = 10 \mu\Omega \cdot \text{cm}$ and of CuPd (A1) $\rho_h = 45 \mu\Omega \cdot \text{cm}$ [25]. Low-temperature annealing below 550°C produces Pd enrichment of the Ag(Pd) phase and thus an increase in resistivity, while conversely, it induces some ordering of the CuPd A1 in B2 and thus a decrease in the resistivity of the overall CuPd phase. The resistivity of the pure B2 phase was measured as $\rho_{B2} = 5 \mu\Omega \cdot \text{cm}$ [26]. As previously mentioned, B2 formation is characterized by a slow kinetics which makes necessary to perform annealing with long enough time for relevant data correlation between alloys having Ag(Pd) with the same Pd content and CuPd with the same fraction of B2. In the following, the electrical conductivity is expressed in % IACS, which is with respect to the international annealed copper standard, having a resistivity of $1.7 \mu\Omega \cdot \text{cm}$. With ρ_s and ρ_h in $\mu\Omega \cdot \text{cm}$, this is obtained by multiplying relation (6) by 170.

Experimental conductivities as a function of the CuPd volume fraction are plotted for the three alloys in the as-processed state and after long term annealing in figures 5a and 5b, respectively. Data fittings with relation (6) allow to obtain the three parameters, A, ρ_s, ρ_h on both curves. Alloys after wire drawing (as-processed) contain Ag(Pd) and CuPd(A1) phases and the fit of the data with relationship (6) (Figure 5a), assuming from [25] that $\rho_s = 10 \mu\Omega \cdot \text{cm}$ and of CuPd (A1) $\rho_h = 45 \mu\Omega \cdot \text{cm}$, gives, $A = 1.49 \pm 0.02 \approx 3/2$. As A is the signature of the microstructure non-ideality (anisotropy shape factor, phase interconnectivity...) it should not change drastically during anneal, meaning it can be fixed for further fitting. So the fit of data of the annealed alloys (figure 5b) to $\rho_s = 12.7 \pm 0.2 \mu\Omega \cdot \text{cm}$ and of CuPd (A1+B2) $\rho_h = 17.4 \pm 0.4 \mu\Omega \cdot \text{cm}$. The model is a perfect periodic packing of the CuPd in Ag(Pd). Comparatively it is intuitively assumed that a random packing offers "short cuts" and higher electrical conductivity. Incidentally, one notices that the geometrical parameter is such that $1/A \approx 2/3$ which is close to the random packing density. For the annealed alloys (figure 5b), as expected, the resistivity of Ag(Pd) increases slightly with the increase in Pd content while the resistivity of CuPd decreases, due to B2 formation at the expense of A1. Owing to a random packing, it is expected parallel contributions of A1 and B2 phases which allows evaluating the B2 fraction in the CuPd phase. Considering a mixing law, $1/\rho_h = \chi_{B2}/\rho_{B2} + (1 - \chi_{B2})/\rho_{A1}$, B2 fraction is estimated in the range of 20% which is in remarkable agreement with TEM observations (figure 1) giving around 10 to 23 %.

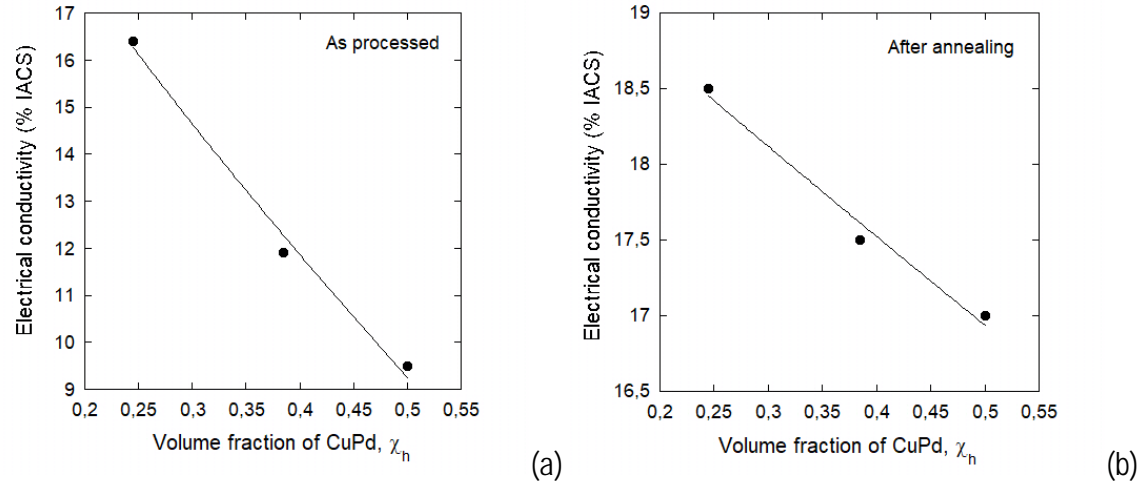


Figure 5 : Experimental electrical conductivity as a function of CuPd volume fraction for alloys (a) as-drawn (b) after long term annealing. Solid lines are the fitting with the relation 6.

Trends in mechanical and electrical properties

From all these analyses and developments, it is now possible to calculate the main trends in electrical conductivity and mechanical strength for predictive purposes. Calculations are made for volume fractions of CuPd phase below 50% (as percolation of Ag(Pd) is necessary for the material to keep plastic ability) and for grain sizes of 20, 40 and 80 nm. Results for the long term annealing case (case 1) are plotted in figure 6a. The Ag(Pd) resistivity is taken to $\rho_s = 12.5 \mu\Omega.cm$ and that of CuPd (mixture A1 and B2) is $\rho_d = 17.15 \mu\Omega.cm$, according to the above fittings. Data corresponding to experimental measurements with grain size of 50 nm and 45 nm (see table 2) are also added. Figure 6b reports the models calculated for an ideal CuPd phase in the B2 form only (case 2), with resistivities $\rho_s = 12.5 \mu\Omega.cm$ and $\rho_h = 5 \mu\Omega.cm$. The opposite trends between the first and second cases should be emphasized, that is a decrease (respectively an increase) in conductivity with increasing mechanical strength which is related to the ratio of resistivity ρ_s/ρ_h which is lower (respectively larger) than unity.

With the objective of improving electrical conductivity while maintaining the mechanical strength, case 1 shows that the strategy is necessarily to decrease the volume fraction of CuPd phase. This would naturally induce a decrease of strength which might be compensated by the reduction of grain size. However, it arises that such a grain refinement should need to be substantial up to the range of 20 nm or less, which would be difficult to obtain by wire drawing. The trend indicates that the maximum possible electrical conductivity is of the order of 20% IACS for case 1. In contrast, the increase of CuPd

B2 phase volume fraction would allow to improve both mechanical strength and electrical conductivity up to a maximum of the order of 30 % IACS. Interestingly, increase in CuPd B2 is accompanied by increase in strength which would allow to increase the grain size to keep a constant strength. Hence, coarser grains would allow to revisit the wire drawing process towards lesser constrain conditions. These results show interesting perspective for the ternary AgCuPd. Nevertheless, it is recalled that whilst the first case is obtained for reasonable thermal (time/temperature) annealing, the second case demands most likely unrealistic long term thermal treatment to obtain the full transformation of CuPd from A1 to B2.

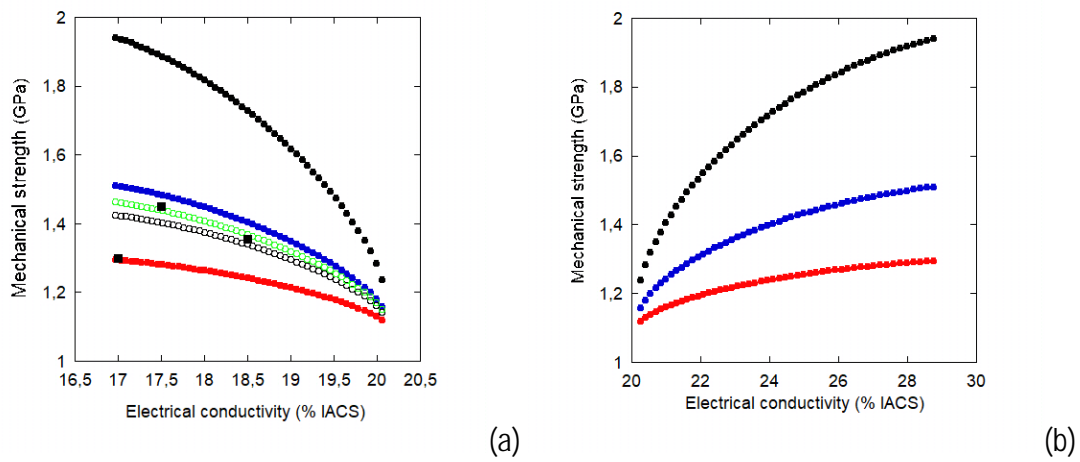


Figure 6: Mechanical strength versus electrical conductivity % IACS modeled for different grain sizes (red 80 nm, blue 40 nm and black 20 nm) (a) for long term annealing, models for grain size of 50 nm, open dots and 45 nm green open dots are added with the 3 experimental data (squares) (b) hypothetical case with CuPd phase in the B2 form.

Conclusion

Complex ternary AgCuPd alloys are studied to evaluate their ability to combine mechanical strength and electrical conductivity for electric and electronic applications. These alloys are formed of Ag(Pd) solid solution and CuPd A1 and B2 phase, which volume fraction depends on thermal treatment.

Phenomenological models are proposed to describe the variations of the mechanical strength and the electrical conductivity as a function of volume fraction of the various phases and the grain size.

Electrical conductivity is obtained from an equivalent electric circuit describing the phase Ag(Pd) and CuPd arrangement in a 3 dimensional checkboard-like structure. A geometric parameter is added to take into account of the random phase distribution in the materials. Mechanical strength modelling was based on a previous analysis of mixing hard and soft phases. The Hall-Petch effect has to be added to

take into account the nanometric grain size and a concept of secondary dislocations pile up (“super dislocation”) is proposed. Modellings are fitted with experimental data of three alloys having different volume phase fractions and grain sizes.

Combining the two models allows to assess trends in terms of mechanical strength and electrical conductivity for the AgCuPd ternary alloy with the following main conclusions:

- Reasonable annealing condition (time / temperature) produces alloys with the ratio of Ag(Pd) – CuPd (A1+B2) resistivity $\rho_s/\rho_h < 1$. Improving electrical conductivity with a maximum value of 20% IACS can be obtained by decreasing CuPd content. This is accompanied by decreasing the mechanical strength partially compensable by grain refinement.
- Appropriate long term annealing increasing CuPd B2 phase is able to turn $\rho_s/\rho_h > 1$ and reversal trend is observed with simultaneous increase of the mechanical strength and electrical conductivity up to 30 % IACS at 50% volume fraction of B2.

Acknowledgement.

This work is part of the PhD thesis of Solène Iruela under the CIFRE contract n° 2017/1134 funded by ANRT and the company METALOR. The authors are indebt to Christine Bourda (METALOR) for support and discussions and Gilles Renou (SIMaP) is deeply acknowledge for assistance in TEM experiments, ACOM analyses and discussions.

The raw/processed data required to reproduce these findings cannot be shared at this time due to technical or time limitations.

References

- [1] X.H. Zhang, Y. Zhang, B.H. Tian, K.X. Song, P. Liu, Y.L. Jia, X.H. Chen, J.C. An, Z. Zhao, Y. Liu, A.A. Volinsky, X. Li, T. Yin, Review of nano-phase effects in high strength and conductivity copper alloys, *Nanotechnol. Rev.* 8(1) (2019) 383-395.
- [2] S.Z. Han, E.A. Choi, S.H. Lim, S. Kim, J. Lee, Alloy design strategies to increase strength and its trade-offs together, *Prog. Mater. Sci.* 117 (2021) 51.
- [3] Y. Champion, Y. Brechet, Effect of Grain Size Reduction and Geometrical Confinement in Fine Grained Copper: Potential Applications as a Material for Reversible Electrical Contacts, *Advanced Engineering Materials* 12(8) (2010) 798-802.
- [4] L. Lu, Y.F. Shen, X.H. Chen, L.H. Qian, K. Lu, Ultrahigh strength and high electrical conductivity in copper, *Science* 304(5669) (2004) 422-426.

- [5] R.K. Islamgaliev, K.M. Nesterov, J. Bourgon, Y. Champion, R.Z. Valiev, Nanostructured Cu-Cr alloy with high strength and electrical conductivity, *Journal of Applied Physics* 115(19) (2014).
- [6] K. Franczak, P. Kwasniewski, G. Kiesiewicz, M. Zasadzinska, B. Jurkiewicz, P. Strzepek, Z. Rdzawski, Research of mechanical and electrical properties of Cu-Sc and Cu-Zr alloys, *Arch. Civ. Mech. Eng.* 20(1) (2020) 15.
- [7] Y.X. Ye, X.Y. Yang, J. Wang, X.K. Zhang, Z.L. Zhang, T. Sakai, Enhanced strength and electrical conductivity of Cu-Zr-B alloy by double deformation-aging process, *Journal of Alloys and Compounds* 615 (2014) 249-254.
- [8] I. Lomakin, M. Castillo-Rodriguez, X. Sauvage, Microstructure, mechanical properties and aging behaviour of nanocrystalline copper-beryllium alloy, *Materials Science and Engineering a-Structural Materials Properties Microstructure and Processing* 744 (2019) 206-214.
- [9] G.L. Xie, Q.S. Wang, X.J. Mi, B.Q. Xiong, L.J. Peng, The precipitation behavior and strengthening of a Cu-2.0 wt% Be alloy, *Materials Science and Engineering a-Structural Materials Properties Microstructure and Processing* 558 (2012) 326-330.
- [10] M.F. Ashby, The deformation of plastically non-homogeneous materials, *Philosophical Magazine* 21 (1970) 399-424.
- [11] L. Perriere, Y. Champion, Phases distribution dependent strength in metallic glass-aluminium composites prepared by spark plasma sintering, *Materials Science and Engineering a-Structural Materials Properties Microstructure and Processing* 548 (2012) 112-117.
- [12] R. Taylor, Transformation in the Copper–Palladium Alloys, *Journal of Institute of Metals* (1934) 255-272.
- [13] A.Y. Volkov, Improvements to the Microstructure and Physical Properties of Pd-Cu-Ag Alloys ENHANCEMENT OF THE MECHANICAL AND ELECTRICAL PROPERTIES, *Platinum Metals Review* 48(1) (2004) 3-12.
- [14] S.J. Andersen, B. Holme, C.D. Marioara, Quantification of small, convex particles by TEM, *Ultramicroscopy* 108(8) (2008) 750-762.
- [15] G. Voyiadjis, M. Yaghoo, *Size Effects in Plasticity. From Macro to Nano*, Elsevier 2020.
- [16] Z. Hashin, S. Shtrikman, A Variational Approach to the Theory of the Effective Magnetic Permeability of Multiphase Materials, *Journal of Applied Physics* 33 (1962) 3125.
- [17] S.Y. Chang, C.F. Chen, S.J. Lin, T.Z. Kattamis, Electrical resistivity of metal matrix composites, *Acta Materialia* 51(20) (2003) 6291-6302.
- [18] F. Lux, MODELS PROPOSED TO EXPLAIN THE ELECTRICAL-CONDUCTIVITY OF MIXTURES MADE OF CONDUCTIVE AND INSULATING MATERIALS, *Journal of Materials Science* 28(2) (1993) 285-301.
- [19] L. Tian, I. Anderson, T. Riedemann, A. Russell, Modeling the electrical resistivity of deformation processed metal-metal composites, *Acta Materialia* 77 (2014) 151-161.
- [20] S.H. Pan, T.L. Wang, K.Y. Jin, X.R. Cai, Understanding and designing metal matrix nanocomposites with high electrical conductivity: a review, *Journal of Materials Science* 57(12) (2022) 6487-6523.
- [21] G.W. Milton, Proof of a conjecture on the conductivity of checkerboards, *J. Math. Phys.* 42(10) (2001) 4873-4882.
- [22] D. Gall, Electron mean free path in elemental metals, *Journal of Applied Physics* 119(8) (2016) 5.
- [23] B.R. Sun, T.D. Shen, Probing the Deformation Mechanisms of Nanocrystalline Silver by In-Situ Tension and Synchrotron X-ray Diffraction, *Metals* 10(12) (2020).
- [24] Y. Champion, L. Perriere, Strain Gradient in Micro-Hardness Testing and Structural Relaxation in Metallic Glasses, *Advanced Engineering Materials* 17(6) (2015) 885-892.
- [25] C.Y. Ho, M.W. Ackerman, K.Y. Wu, T.N. Havill, R.H. Bogaard, R.A. Matula, S.G. Oh, H.M. James, ELECTRICAL-RESISTIVITY OF 10 SELECTED BINARY ALLOY SYSTEMS, *J. Phys. Chem. Ref. Data* 12(2) (1983) 183-322.
- [26] S. Iruela, Optimisation par voie métallurgique des performances mécanique et électrique d'alliages de métaux nobles, Université Grenoble Alpes, Grenoble, 2021.